

A New Continuous Optimization Method for Mixed Integer Space Travelling Salesman Problem

Liqiang Hou · Shufan Wu · Zhongcheng Mu · Meilin Liu

Received: date / Accepted: date

Abstract The travelling salesman problem (TSP) of space trajectory design is complicated by its complex structure design space. The graph based tree search and stochastic seeding combinatorial approaches are commonly employed to tackle the time-dependent TSP due to their combinatorial nature. In this paper, a new continuous optimization strategy for the mixed integer combinatorial problem is proposed. The space trajectory combinatorial problem is tackled using continuous gradient based method. A continuous mapping technique is developed to map the integer type ID of targets on the sequence to a set of continuous design variables. Expected flyby targets are introduced as references and used as priori to select the candidate target to fly by. Bayesian based analysis is employed to model accumulated posterior of the sequence and a new objective function with quadratic form constraints is constructed. The new introduced auxiliary design variables of expected targets together with the original design variables are set to be optimized. A gradient based optimizer is used to search optimal sequence parameter. Performances of the proposed algorithm are demonstrated through a multiple debris rendezvous problem and a static TSP benchmark.

Keywords Space trajectory design · Combinatorial optimization · Debris removal · Gradient based optimization · Bayesian inference

Liqiang Hou
School of Aeronautics and Astronautics, Shanghai Jiaotong University, Shanghai, China,
200240
E-mail: houliqiang@sjtu.edu.cn

Shufan Wu, Zhongcheng Mu, Meilin Liu
School of Aeronautics and Astronautics, Shanghai Jiaotong University, Shanghai, China,
200240

1 Introduction

Combinatorial optimization of space trajectory design finds an optimal sequence of the objects from a finite set of objects. The searching process of combinatorial optimization operates on discrete feasible solutions. Typical problems involving combinatorial optimization are the travelling salesman problem (TSP), the minimum spanning tree problem (MST), and the knapsack problem. Different to the common design problems of the space design, in combinatorial optimization of trajectory design a number of sequences are selected and optimized. For each sequence, a global optimization problem is solved in order to search the optimal continuous parameters.

The optimization considers not only the continuous design parameters, e.g. launch time, fuel consumption, impulsive velocity increment, time of flight of the transfers between objects, etc., but the discrete parameters, such as the celestial bodies and debris to flyby or rendezvous. One needs to explore not only the continuous design space to search the optimal orbital transfer parameters, but the set of discrete items of the targets to be visited. The design space of the continuous design space is thus separated by the discrete candidate target set. One needs to decide the targets to be visited, and the order of targets.

Although strict tree enumeration is a practical scheme for small-scale space trajectory planning, in many such problems, exhaustive search is not tractable. Complexity of the search scheme quickly becomes intractable for the problems with even moderately sized candidate set. The most challenging aspect of combinatorial optimization of space trajectory design are from the combinatorial part, i.e. the policy of selection of the candidate objects to construct the sequence.

To tackle the issues due to the problem's combinatorial nature, one can discretize or branch the continuous design space into a set of separated continuous subspace. Each subspace are associated to a set of candidates using specific decision making policy. Graph based search strategies such as branch-and-bound tree searches are then used to search optimal sequence. **It recursively splits the search space into smaller spaces associated to subset of the candidates, and performs a top-down recursive search through the tree of instances formed by the branch operation. Exploration and exploitation of the tree can be improved by introducing a knowledge based pruning criterion preventing nodes to be further expanded.** A notable example of tree searches with heuristic-based pruning, implementing problem knowledge, is the software STOUR of automated design of trajectories with multiple fly-bys designed by Jet Propulsion Laboratory [16], which has been used in several important mission design works [11][19].

Studies in biological social action have always been a great source of inspiration of the mixed integer combinatorial space mission design. Attempts using bio-inspired methodology, such as Ant Colony Optimization (ACO) [4], Genetic Algorithm (GA) [6][10][14], tree search strategies[20] are made to advance automatic planning of the combinatorial search paradigms. Problem

knowledge are used to define heuristics and tune of the internal parameters for different data sets or domains.

The ant colony meta heuristic and its variants have been successfully applied in a variety of space optimization problems. **The Physarum and the ACO variants model the discrete decision making problems into a decision graph, and unvisited node is stochastically selected with probability** [26][24][4]. Stuart et al. use a modified ACO suitable for smooth solution spaces to generate asteroid tours [26]. The route-finding ant colony optimization algorithm is incorporated into the automated tour-generation procedure for the sun-Jupiter Trojan asteroids. ACO routing algorithm and multi-agent coordination via auctions are incorporated into a debris mitigation tour scheme design [25]. In [4], an ant colony systems is used to solve MGAP design. In [24], hybridization between Beam Search and the population-based ACO is proposed to tackle the combinatorial problem of finding the ideal sequence of bodies.

Approaches employing seeding based genetic algorithms are also proven effective in searching the optimal sequence [17][9]. Abdelkhalik et al. solve the multiple-flyby problem with impulsive chemical thrust using a single genetic algorithm (GA) [1]. Nyew et al. proposed a structured-chromosome evolutionary algorithms for variable-size autonomous interplanetary trajectory planning optimization [18]. In [10], the problem is approached by using Hidden Genes Genetic Algorithms (HGGA) where each sequence is represented by a binary chromosome. **In multi-objective TSP with NSGA-II [7], a representation scheme is used to adapt the mixed integer decision variables to the NSGA-II framework. A 11-bit strings is designed to represent which and how many planets are used in the trajectory optimization.**

Other applications of metaheuristic algorithms in the path planning include: multi-objective particle swarm [5][29], simulated annealing [3]. [28][8] uses inspiration from the behavior of a simple amoeboid organism, the Physarum Polycephalum, that is endowed by nature with simple heuristics that can solve complex discrete decision making problems .

Some relatively recent works on discrete combinatorial problems of space trajectory design employ artificial intelligence and machine learning. Tsirogianis, George A proposed an automatic planing approach using artificial intelligence and machine learning [27]. In [12], a heuristic-free approach using Monte Carlo Tree Search (MCTS) is proposed for the automated encounter sequence planning. Problem-specific modifications are made to adapt traditional MCTS to trajectory planning of the Rosetta and Cassini-Huygens interplanetary mission design. Four steps, namely: selection, expansion, simulation, and back-propagation, are performed iteratively till the stopping criteria are met [2].

It can be seen that, though numerous methods and algorithms are developed to tackle the space trajectory combinatorial optimization problem, either the graph based approach or the bio-inspired and artificial intelligence based approaches, the discretization based searching strategy is used in natural. Feasible space of the continuous parameters are discretized to construct branches and offspring associated to set of candidates. Policies such as bio-inspired social

actions or population based evolutionary strategies are then used to generate and select the offspring or branches to be explored. The procedure is iteratively implemented till the optimal sequence is obtained.

Some recent research works developed continuous representation techniques in combinatorial optimization. Pichugina et.al proposed a continuous presentation and functional extensions in combinatorial optimization. Functional representations of the Boolean set, general permutation, and poly permutation sets are derived[22]. In [21], a continuous representation technique in combinatorial optimization is proposed based on algebraic-topological features of the sets and properties of functions over them.

In this work, a new strategy for the sequence optimization is developed and tested. Different to the commonly used combinatorial optimization algorithms, a continuous gradient based optimizer for the space trajectory TSP is developed. Candidates of the objects are associated to a set of continuous characteristic parameters, and a continuous mapping technique is developed to map the discrete or mixed integer combinatorial problem into a continuous quadratic-like optimization problem. Unlike the common combinatorial optimization algorithm, at each node of the sequence, a single candidate is selected and associated to a metric value, no branch and pruning operation is implemented. A gradient based continuous optimizer is used to search optimal sequence. Effectiveness of proposed method are demonstrated through a static TSP benchmark and multiple debris rendezvous problem .

The remainder of the paper is structured as follows. Section 2 outlines the combinatorial space trajectory design and TSP of multiple debris rendezvous. The continuous mapping approach is modelled and presented in Section 3. Section 4 presents tests of a static TSP benchmark using proposed method. Results of numerical simulation of the multiple debris rendezvous are presented in Section 5. Section 6 concludes the paper and describe future work.

2 Problem statement

2.1 TSP in Space Mission Design

The TSP in space mission design optimizes orbital transfer parameters and the sequence of objects to fly by. The solution space is defined by the launch date T_0 and times of flight (TOF) from one object to the subsequent one, T_i . The total cost of the multiple transfer can thus be described as

$$J = \sum_{k=1}^N y(T_k, \mathcal{I}_k, \mathbf{d}_k) \quad (1)$$

s.t.

$$\mathbf{s}_k = \mathbf{g}(\mathbf{s}_{k-1}) \quad (2)$$

$$\mathbf{x}_k = \mathbf{f}(\mathbf{x}_{k-1}) \quad (3)$$

$$\mathbf{z}_k = \mathbf{H}\mathbf{x}_k \quad (4)$$

where $\mathcal{I}_k \in \mathbb{Z}$ represents the target body, N is the number of targets. \mathbf{d}_k is continuous design variables associated to the k -th transfer, e.g., relevant dates, magnitude and orientation of impulse velocities etc. $y(\cdot)$ is the cost function of the k -th transfer, \mathbf{s} are state of spacecraft e.g. position, velocity or orbital elements. \mathbf{x}_k and \mathbf{z}_k are state and observation of the characteristic parameters of \mathcal{I}_k respectively. $\mathbf{f}(\cdot)$, $\mathbf{g}(\cdot)$ are state equations of \mathcal{I}_k and the spacecraft, and $\mathbf{h}(\cdot)$ is observation equation of \mathcal{I}_k .

The problem is a mixed integer combinatorial optimization problem. Optimization of the TSP is annoyed by its complex structured search spaces. One needs to explore not only the design space of the orbital transfer parameters, but the discrete candidate set $\mathbf{I} \in \mathbb{Z}^N$.

The combination of the discrete set and continuous transfer parameters partitions the whole feasible solution space into a set of separately distributed subspace. Algorithms using different policies to generate and determine the optimal sequence are therefore developed. Though efforts are made to improve the searching process, computational cost of the TSP solvers with even middle sized candidates is expensive. Since the time-dependent TSP is complicated by the discrete candidate set, if an equivalent continuous search space with continuous gradient for the TSP can be given, optimization of the problem will be much easier, and corresponding computational cost will be greatly reduced.

2.2 Time-dependent TSP of multiple debris rendezvous

Consider a removal sequence problem of Sun-synchronous, Low-Earth-Orbit debris. Data set of the debris parameters are from the 9th Global Trajectory Optimisation Competition (GTOC9) [13]. Inclinations and semi-major axes of the debris objects are about $96^\circ - 101^\circ$ and about 600 – 900 km larger than the Earth's radius respectively. Eccentricity of the debris ranges from about 0.02 down to almost zero. The task is to design a series of transfers to remove a set of orbiting debris.

2.2.1 Problem statement

Objective of the multiple debris rendezvous is to minimize

$$J = \sum_{i=1}^N \Delta v_i \quad (5)$$

where Δv_i is the cost of impulsive transfer to rendezvous the i -th debris.

After the rendezvous, the spacecraft stays in proximity of the debris for 5 days for the removal operation and start a new transfer for the next rendezvous. Precession rates of the debris considering J2 coefficient given the

orbital element $a, e, i, \Omega, \omega, M$ are computed as

$$\dot{\Omega} = -\frac{3}{2}J_2 \left(\frac{r_{eq}}{p}\right)^2 n \cos i \quad (6)$$

$$\dot{\omega} = \frac{3}{4}J_2 \left(\frac{r_{eq}}{p}\right)^2 n(5 \cos^2 i - 1) \quad (7)$$

where r_{eq} is mean radius of equator, $n = \sqrt{\frac{\mu}{a^3}}$ is mean motion, and p is semilatus rectum and computed as $p = a(1 - e^2)$.

Corresponding right ascension of the ascending node, Ω , argument of perigee, ω and the mean anomaly M at epoch t are

$$\Omega - \Omega_0 = \dot{\Omega}(t - t_0) \quad (8)$$

$$\omega - \omega_0 = \dot{\omega}(t - t_0) \quad (9)$$

$$M - M_0 = n(t - t_0) \quad (10)$$

Initial values of the debris ephemerides, $[a_0, e_0, i_0, \Omega_0, \omega_0, M_0]$ and initial epoch t_0 are taken from the GTOC-9 database.

Cartesian form Ordinary Differential Equations (ODEs) of spacecraft's and debris' motion is given by the following set of equations

$$\ddot{x} = -\frac{\mu x}{r^3} \left\{ 1 + \frac{3}{2}J_2 \left(\frac{r_{eq}}{r}\right)^2 \left(1 - 5\frac{z^2}{r^2}\right) \right\} \quad (11)$$

$$\ddot{y} = -\frac{\mu y}{r^3} \left\{ 1 + \frac{3}{2}J_2 \left(\frac{r_{eq}}{r}\right)^2 \left(1 - 5\frac{z^2}{r^2}\right) \right\} \quad (12)$$

$$\ddot{z} = -\frac{\mu z}{r^3} \left\{ 1 + \frac{3}{2}J_2 \left(\frac{r_{eq}}{r}\right)^2 \left(3 - 5\frac{z^2}{r^2}\right) \right\} \quad (13)$$

where r is the radius, $[x, y, z]$ and $[\dot{x}, \dot{y}, \dot{z}]$ are position and velocity respectively. Table 1 summarizes constants of the numerical integrator and computation of ephemerides of the debris.

Table 1 Values of problem constants

	Value	Unit
μ	398600.4418	km ³ /sec ²
J_2	1.08262668e-3	
r_{eq}	6378.137	km

2.2.2 Cost of near-circular impulsive orbital transfer

Suppose the initial element of spacecraft at time t_0 is $\boldsymbol{\sigma}_0 = [a_0, e_0, i_0, \Omega_f, \omega_0, M_0]$, the Δv for spacecraft fly to and rendezvous the target with orbital element $\boldsymbol{\sigma}_f = [a_f, e_f, i_f, \Omega_f, \omega_f, M_f]$ after time of flight Δt can be approximately computed as

$$\Delta V_a = \frac{1}{2} \frac{\Delta a}{a_0} V_0 \quad (14)$$

$$\Delta V_e = \frac{1}{2} \Delta e V_0 \quad (15)$$

$$\Delta V_i = 2V_0 \sin\left(\frac{\Delta i}{2}\right) \quad (16)$$

$$\Delta V_\Omega = \sin i_0 \Delta \Omega V_0 \quad (17)$$

where V_0 is the spacecraft's velocity

$$V_0 = \sqrt{\frac{\mu}{a_0}} \quad (18)$$

and

$$\Delta a = |a_0 - a_f| \quad (19)$$

$$\Delta e = |e_0 - e_f| \quad (20)$$

$$\Delta i = |i_0 - i_f| \quad (21)$$

$$\Delta \Omega = |(\Omega_f + \dot{\Omega}_f \Delta t) - (\Omega_0 + \dot{\Omega}_0 \Delta t)| \quad (22)$$

where the drift rate of ascending node considering J2 impacts, $\dot{\Omega}_f$ and $\dot{\Omega}_0$ is computed using eq.6.

The total cost of the transfer is

$$\Delta V = \sqrt{\Delta V_a + \Delta V_e + \Delta v_i + \Delta V_\Omega} \quad (23)$$

2.2.3 Reformulate the multiple rendezvous problem into a continuous optimization problem

The optimization problem minimizes the total cost of ΔV_k and determine the optimal sequence \mathcal{I}_k . The mixed integer design vector of the optimization is $\{T_k, \mathcal{I}_k\}$, where T_k is the ToF of the k -th transfer. To associate the integer \mathcal{I}_k to continuous parameters, an expected debris $\bar{\mathcal{I}}_k$ is defined using $\boldsymbol{\mu}_{k-1} = [\mu_a, \mu_e, \mu_i, \mu_o]_{k-1}$ and $\boldsymbol{\Sigma}_{k-1} = \text{diag}[\sigma_a, \sigma_e, \sigma_i, \sigma_o]_{k-1}$. Initial value of $\boldsymbol{\mu}_{k-1}$ is set to differences of the orbital elements of \mathcal{I}_k^* with respect to those of spacecraft at the $k-1$ -th node. Observation of \mathcal{I}_k is defined as $\mathbf{z}_k = [\Omega_k]$, as the ascending node Ω_k is coupled closely to variation of the orbital parameters a, e , and i .

Design parameters of the continuous problem consist of $\{\mathcal{I}_k, \boldsymbol{\mu}_{k-1}, \boldsymbol{\Sigma}_{k-1}, \kappa_k\}$, where κ_k is slack variable for the inequality constraint. The target \mathcal{I}_k is selected using \mathbf{z}_k , and priori of $\boldsymbol{\mu}_{z,k}$ and $\boldsymbol{\Sigma}_{z,k}$ of $\tilde{\mathcal{I}}_k$. Compute Δv_k to the debris \mathcal{I}_k , likelihood of the transfer $\mathcal{L}(\Delta v_k | \mathcal{I}_k)$ can then be computed with respect to $\mu_{v,k}$ and $\sigma_{v,k}$ of \mathcal{I}_k^* . Objective function value of the total cost with accumulated posterior constraints is computed using eq.54.

3 Mapping discrete design parameters of TSP into continuous design space

In state equation and observation equation of flyby target (eq.3-eq.4), the state \mathbf{x}_k and observation \mathbf{z}_k is associated and varied with \mathcal{I}_k . Conventional TSP methods select the candidate \mathcal{I}_k directly from the integer type data set \mathbf{I} using a specific policy. Position and velocity of the object is then computed and substituent into the cost function to compute the total cost of the transfer. Selection and decision policy of the candidate \mathcal{I}_k is analyzed and updated according to the total cost obtained. The strategy works successfully in many space TSP optimization scenarios. However, as analyzed in preceding sections, discrete tree and string like structures have to be constructed and associated to the flyby targets. One have to examine each feasible subspace separately, no gradient of the trajectory variation of the spacecraft and flyby target is used to accelerate the searching process.

Instead of using integer type ID to represent the flyby target, in this work, a new set of continuous characteristic parameters are used to define the flyby target. Expected flyby target $\tilde{\mathcal{I}}_k$ of the sequence are introduced, and a continuous probabilistic metric with respect to expected $\tilde{\mathcal{I}}_k$ is used to select the flyby target. Accumulated probabilistic metric value of the transfers are computed and set as constraints of the optimization.

3.1 Associate integer ID to continuous characteristic parameters

Suppose at the $k-1$ -th node, the state of spacecraft is \mathbf{s}_{k-1} . Initial value of the state of expected $\tilde{\mathcal{I}}_k$ is \mathbf{x}_{k-1} and normally distributed with $\mathcal{N}(\boldsymbol{\mu}_{k-1}, \boldsymbol{\Sigma}_{k-1})$. Expected value and covariance of the state of $\tilde{\mathcal{I}}_k$ at the k -th node can be predicted and expressed as $\boldsymbol{\mu}_{k|k-1}$ and $\boldsymbol{\Sigma}_{k|k-1}$ respectively.

Given the predicted $\boldsymbol{\mu}_{k|k-1}$ and $\boldsymbol{\Sigma}_{k|k-1}$, expected value of the observation of $\tilde{\mathcal{I}}_k$ at the k -th node can be predicted as $\boldsymbol{\mu}_{z,k}$ and $\boldsymbol{\Sigma}_{z,k}$. A flyby target \mathcal{I}_k can then be selected with respect to \mathcal{I}_k^* using the characteristic parameter. Priori of the candidate \mathcal{I}_k , or the probability of \mathcal{I}_k to be selected is given as

$$P(\mathcal{I}_k | \mathcal{I}_k^*) = \mathcal{N}(\mathbf{z}_k | \boldsymbol{\mu}_{z,k}, \boldsymbol{\Sigma}_{z,k}) \quad (24)$$

where $\mathbf{z}_k = h(\mathbf{x}_k)$ is characteristic parameters of \mathcal{I}_k at the k -th node respectively.

Compute the probability level of each candidate $\mathcal{I}_k \in \mathbf{I}$ using eq.24, and save it in the data set of priori list for selection. Selection of \mathcal{I}_k is now associated to the probability level computed using a set of continuous parameters.

Response of the selection of \mathcal{I}_k is also supposed to be Gaussian. Given the target \mathcal{I}_k , likelihood of the cost to \mathcal{I}_k can be compute as

$$\mathcal{L}(y_k|\mathcal{I}_k) = \mathcal{N}(y_k|\mu_{y,k}, \sigma_{y,k}) \quad (25)$$

where y_k is the cost to \mathcal{I}_k , μ_y and σ_y are expected value and variance of the cost of the k -th transfer.

With new introduced expected \mathcal{I}_k^* , selection of the target \mathcal{I}_k and corresponding impacts on the cost of transfer can be rewritten as a continuous problem. Probability level of the transfer given the auxiliary characteristic parameters can be computed and measured. The original deterministic objective function can then be reformulated into an optimization problem that minimizes the total cost of transfer while at the same time maximizes its accumulated probability level. This can be done by the following strategy.

3.2 Bayesian Inference

Eq.25 shows likelihood of the cost y_k given the priori of \mathcal{I}_k . With the priori and likelihood, posterior of the transfer can be computed using Bayesian theorem

$$\pi(y_k) \propto \mathcal{L}(y_k|\mathcal{I}_k)P(\mathcal{I}_k|\mathcal{I}_k^*) \quad (26)$$

Accumulated logarithm of the posterior for the TSP scheming is

$$\begin{aligned} \sum_{k=1}^N \log \pi(y_k) = & - \sum_{k=1}^N (\mathbf{z}_k - \boldsymbol{\mu}_{z,k}) \boldsymbol{\Sigma}_{z,k}^{-1} (\mathbf{z}_k - \boldsymbol{\mu}_{z,k})^T \\ & - \sum_{k=1}^N (y_k - \mu_{y,k}) \boldsymbol{\Sigma}_{y,k}^{-1} (y_k - \mu_{y,k})^T + (\cdot) \end{aligned} \quad (27)$$

where (\cdot) represents the logarithm term of

$$- \frac{1}{2} \log(2\pi) - \frac{1}{2} \ln(|\boldsymbol{\Sigma}_{y,k}|) - \frac{1}{2} \ln(|\boldsymbol{\Sigma}_{z,k}|) - \frac{n_z}{2} \ln(2\pi) \quad (28)$$

and can be removed during the optimization if the variance of y and \mathbf{z} is small. The accumulated posterior includes the most current observation of the cost y_k , minimizing the value will allow us to move the samples in the prior to regions of high likelihood.

Figure 1 shows priori and likelihood of the expected \mathcal{I}_k^* and flyby \mathcal{I}_k . First, an expected \mathcal{I}_k^* is initialized and propagated to t_k . A flyby target \mathcal{I}_k at t_k is then selected from the data set using the priori. Corresponding cost to \mathcal{I}_k is then computed. Posterior of the selection of \mathcal{I}_k is computed using Bayesian theorem. Finally, a new objective function is defined to minimize the total cost of the transfer, while at the same to maximize the accumulated posterior.

$$J = \min \sum_{k=1}^N y_k \quad (29)$$

s.t.

$$\begin{aligned} \min \Pi = & \sum_{k=1}^N (\mathbf{z}_k - \boldsymbol{\mu}_{z,k}) \boldsymbol{\Sigma}_{z,k}^{-1} (\mathbf{z}_k - \boldsymbol{\mu}_{z,k})^T \\ & + \sum_{k=1}^N (y_k - \boldsymbol{\mu}_{y,k}) \boldsymbol{\Sigma}_{y,k}^{-1} (y_k - \boldsymbol{\mu}_{y,k})^T \end{aligned} \quad (30)$$

3.3 Propagation of the expected values and covariance

In the equations of priori and likelihood, several covariance of \mathcal{I}_k and \mathcal{I}_k^* , such as $\boldsymbol{\Sigma}_{k|k-1}$, $\boldsymbol{\Sigma}_{z,k}$, $\boldsymbol{\Sigma}_{y,k}$ are involved and computed. The covariance are computed as follows.

Given initial value of \mathcal{I}_k^* at the $k-1$ th node, $\boldsymbol{\mu}_{k-1}$ and $\boldsymbol{\Sigma}_{k-1}$, expected value of \mathcal{I}_k at the k -th node can be predicted as

$$\boldsymbol{\mu}_{k|k-1} = \mathbf{f}(\boldsymbol{\mu}_{k-1}) \quad (31)$$

Predict of the covariance of \mathcal{I}_k^* at the k th node can be obtained using the first order approximation

$$\boldsymbol{\Sigma}_{k|k-1} = \mathbf{F}_{k|k-1} \boldsymbol{\Sigma}_{k-1} \mathbf{F}_{k|k-1}^T \quad (32)$$

where $\mathbf{F}_{k|k-1}$ is the Jacobian of state equation

$$\mathbf{F}_{k|k-1} = \begin{bmatrix} \frac{\partial f_1}{\partial x_1} & \frac{\partial f_1}{\partial x_2} & \cdots & \frac{\partial f_1}{\partial x_n} \\ \vdots & & \ddots & \vdots \\ \frac{\partial f_n}{\partial x_1} & \frac{\partial f_n}{\partial x_2} & \cdots & \frac{\partial f_n}{\partial x_n} \end{bmatrix}_{\mathbf{x}=\mathbf{x}_{k-1}} \quad (33)$$

Accordingly, $\boldsymbol{\mu}_{z,k|k-1}$ and $\boldsymbol{\Sigma}_{z,k|k-1}$ of expected \mathcal{I}_k^* using the observation of characteristic parameters is

$$\boldsymbol{\mu}_{z,k} = \mathbf{h}(\boldsymbol{\mu}_{k|k-1}) \quad (34)$$

$$\boldsymbol{\Sigma}_{z,k} = \mathbf{H}_k \boldsymbol{\Sigma}_{k|k-1} \mathbf{H}_k^T \quad (35)$$

where $\mathbf{H}_{k|k-1}$ is the Jacobian of observation equation

$$\mathbf{H}_k = \begin{bmatrix} \frac{\partial h_1}{\partial x_1} & \frac{\partial h_1}{\partial x_2} & \cdots & \frac{\partial h_1}{\partial x_n} \\ \vdots & & \ddots & \vdots \\ \frac{\partial h_n}{\partial x_1} & \frac{\partial h_n}{\partial x_2} & \cdots & \frac{\partial h_n}{\partial x_n} \end{bmatrix}_{\mathbf{x}=\boldsymbol{\mu}_{k|k-1}} \quad (36)$$

With the value of $\boldsymbol{\mu}_{k|k-1}, \boldsymbol{\Sigma}_{k|k-1}$, estimates of $\boldsymbol{\mu}_{y,k|k-1}$ $\boldsymbol{\Sigma}_{y,k|k-1}$ fly to expected flyby target \mathcal{I}_k^* can be computed as

$$\boldsymbol{\mu}_{y,k|k-1} = y(\boldsymbol{\mu}_{k|k-1}) \quad (37)$$

$$\boldsymbol{\Sigma}_{\mathbf{y},k|k-1} = \mathbf{Y}_k \boldsymbol{\Sigma}_{\mathbf{k}-1} \mathbf{Y}_k^T \quad (38)$$

where

$$\mathbf{Y}_{k|k-1} = \left[\frac{\partial y}{\partial x_1} \quad \frac{\partial y}{\partial x_2} \quad \cdots \quad \frac{\partial y}{\partial x_n} \right]_{\mathbf{x}=\mathbf{x}_{k-1}} \quad (39)$$

Since the cost y_k to actual \mathcal{I}_k is computed and selected using the new observation \mathbf{z}_k , the following equation can be used to update covariance and expected value of y_k given $\boldsymbol{\mu}_{z,k}$ and $\boldsymbol{\Sigma}_{z,k}$.

Given jointly Gaussian \mathbf{z}, \mathbf{y} , one have

$$\begin{bmatrix} y_k \\ \mathbf{z}_k \end{bmatrix} \sim \mathcal{N} \left(\begin{bmatrix} \boldsymbol{\mu}_{y,k} \\ \boldsymbol{\mu}_{z,k} \end{bmatrix}, \begin{bmatrix} \boldsymbol{\Sigma}_y & \boldsymbol{\Sigma}_{yz} \\ \boldsymbol{\Sigma}_{yz} & \boldsymbol{\Sigma}_z \end{bmatrix} \right) \quad (40)$$

where

$$\boldsymbol{\Sigma}_{z,k} = \mathbf{H}_k \boldsymbol{\Sigma}_{k|k-1} \mathbf{H}_k^T \quad (41)$$

$$\boldsymbol{\Sigma}_{yy,k} = \mathbf{Y}_k \boldsymbol{\Sigma}_{k|k-1} \mathbf{F}_k^T \quad (42)$$

$$\boldsymbol{\Sigma}_{yz,k} = \mathbf{Y}_k \boldsymbol{\Sigma}_{k|k-1} \mathbf{H}_k^T \quad (43)$$

$$\boldsymbol{\Sigma}_{zy,k} = \mathbf{H}_k \boldsymbol{\Sigma}_{k|k-1} \mathbf{F}_k^T \quad (44)$$

Estimated expected value and covariance of y_k given the observation of \mathbf{z}_k can be computed as

$$\boldsymbol{\mu}_{y,k} = \boldsymbol{\mu}_{y,k|k-1} + \boldsymbol{\Sigma}_{yz} \boldsymbol{\Sigma}_{zz}^{-1} (\mathbf{z}_k - \boldsymbol{\mu}_{z,k|k-1}) \quad (45)$$

$$\boldsymbol{\Sigma}_{y,k} = \boldsymbol{\Sigma}_{y,k|k-1} - \boldsymbol{\Sigma}_{yz} \boldsymbol{\Sigma}_{zz}^{-1} \boldsymbol{\Sigma}_{zy} \quad (46)$$

3.4 An alternative method for the covariance computation

An alternative to the method of covariance update is using the scaled unscented transform (SUT) [15], which may give more exact results for large levels of the uncertainty but typically requires more computation time. With the method, predict of the mean value and covariance of \mathbf{x} and \mathbf{y} are computed

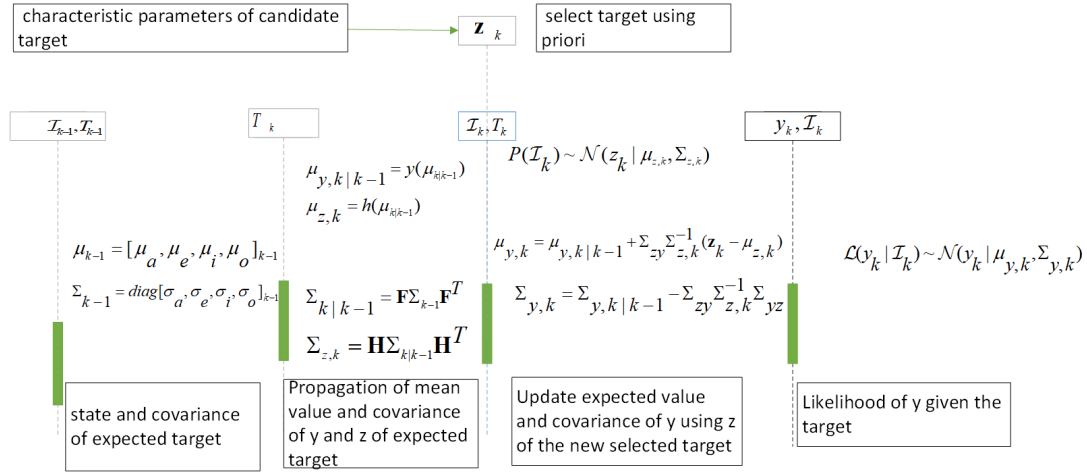


Fig. 1 Priori and likelihood of selecting \mathcal{I}_k . \mathcal{I}_k is selected using characteristic parameters \mathbf{z} with respect to $\mu_{z,k}$ and $\Sigma_{z,k}$. Likelihood of y is modeled and updated using the predicted mean value and covariance of y given \mathcal{I}_k , and \mathbf{z}_k of the selected \mathcal{I}_k .

as weighted sum of the sample function values of specified sigma points

$$\bar{\mathbf{x}} = \sum_{i=1}^r w_i \boldsymbol{\chi}_i \quad (47)$$

$$\Sigma_{\mathbf{x}} = \sum_{i=1}^r w_i (\boldsymbol{\chi}_i - \bar{\mathbf{x}}) (\boldsymbol{\chi}_i - \bar{\mathbf{x}})^T \quad (48)$$

$$\bar{\mathbf{y}} = \sum_{i=1}^r w_i \mathbf{y}_i \quad (49)$$

$$\Sigma_{\mathbf{y}} = \sum_{i=1}^r w_i (\mathbf{y}_i - \bar{\mathbf{y}}) (\mathbf{y}_i - \bar{\mathbf{y}})^T \quad (50)$$

$$\Sigma_{\mathbf{xy}} = \sum_{i=1}^r w_i (\boldsymbol{\chi}_i - \bar{\mathbf{x}}) (\mathbf{y}_i - \bar{\mathbf{y}})^T \quad (51)$$

where w_i is the weight for the sampled points, $\boldsymbol{\chi}_i$ and \mathbf{y}_i are sampled sigma points and corresponding function values.

3.5 Chi-square threshold

In the searching procedure, the stochastic based computation and analysis are used and implemented. Though the new objective function, eq.29-eq.30 looks deterministic, the guess of \mathcal{I}_k at each node is generated scholastically in essence (eq.24).

Consider the quadratic form cost function, eq.30, since the guess of \mathcal{I}_k is generated normally, the quadratic part is also randomly distributed because of the priori of \mathcal{I}_k , and follow a chi-square distribution

$$(\mathbf{z}_k - \boldsymbol{\mu}_{z,k}) \boldsymbol{\Sigma}_{z,k}^{-1} (\mathbf{z}_k - \boldsymbol{\mu}_{z,k})^T + (y_k - \mu_{y,k}) \boldsymbol{\Sigma}_{y,k}^{-1} (y_k - \mu_{y,k})^T \sim \chi_n^2 \quad (52)$$

where $n = n_z + n_y$ is degrees of freedom of chi-square distribution, and n_z and n_y are dimensionality of the characteristic parameters and cost function value respectively.

A chi-square constraint can then be given as

$$(\mathbf{z}_k - \boldsymbol{\mu}_{z,k}) \boldsymbol{\Sigma}_{z,k}^{-1} (\mathbf{z}_k - \boldsymbol{\mu}_{z,k})^T + (y_k - \mu_{y,k}) \boldsymbol{\Sigma}_{y,k}^{-1} (y_k - \mu_{y,k})^T > \chi_n^2(\alpha) \quad (53)$$

where α is the confidence level to be met, e.g. 0.98.

Rewrite the constrained optimization problem into unconstrained form, one have

$$\min_{\mathbf{D}} J = \sum_{k=1}^N [y_k + \kappa_i \max(0, c_k)] \quad (54)$$

$$c_k = (\mathbf{z}_k - \boldsymbol{\mu}_{z,k}) (\boldsymbol{\Sigma}_{z,k} + \mathbf{A})^{-1} (\mathbf{z}_k - \boldsymbol{\mu}_{z,k})^T + (y_k - \mu_{y,k}) \sigma_{y,k}^{-1} (y_k - \mu_{y,k})^T - \chi_n^2(\alpha) \quad (55)$$

where $\mathbf{A} = \text{diag}(\boldsymbol{\epsilon})$, κ_i is slack variable, and \mathbf{D} is design parameters of the new objective function

$$\mathbf{D} = \{T_k, \mathbf{d}_k, \mu_{k-1}, \boldsymbol{\Sigma}_{k-1}, \kappa_k\} \quad (56)$$

in which $\mu_k, \boldsymbol{\Sigma}_k$ are the continuous auxiliary design variables of $\bar{\mathcal{I}}_k$, \mathbf{d}_k is original continuous design variables of the TSP.

The new objective function incorporates statistical features of the expected $\bar{\mathcal{I}}_k$, and the original cost function, and is reformulated into a continuous optimization problem associated to a probability space. The objective is to search the optimal solution of sequence that has lowest cost at maximum probability level. A gradient based optimizer can be used to search iteratively the characteristic parameters of $\bar{\mathcal{I}}_k$ till the chi-square threshold is achieved.

3.6 Searching optimal TSP sequence using gradient based optimizer

In the selection using priori, \mathcal{I}_k is randomly selected with respect to the spacecraft and expected $\bar{\mathcal{I}}_k$. Though the operation is similar to many probabilistic heuristic algorithms for the combinatorial optimization, several features of the proposed algorithm distinguish it from them and make it high efficient in searching the optimal sequence.

With the new strategy, continuous gradient information of the accumulate logarithm probabilistic level of \mathcal{I}_k with respect to expected $\bar{\mathcal{I}}_k$ can be computed and used. No branch operation is required during the search. In the population based methods in which the probabilistic heuristics with the string like structured samples are used and analyzed to to obtain heuristics

for the new individuals. In the new algorithm, only one candidate is selected at each node. The computation is implemented sequentially. No population based sampling and seeding is required.

The algorithm works as follows. First, initial values of the characteristic parameters, $\boldsymbol{\mu}_{k-1}$ and $\boldsymbol{\Sigma}_{k-1}$ are given to initialize the expected $\bar{\mathcal{I}}_k$. State equation of the spacecraft and flyby target are used to propagate the characteristic parameters. Select \mathcal{I}_k from the candidate set using the observations with the priori of $\boldsymbol{\mu}_{z,k}$ and $\boldsymbol{\Sigma}_{z,k}$. Compute expected value and covariance of the cost, $\boldsymbol{\mu}_{y,k}$ and $\boldsymbol{\Sigma}_{y,k}$. Slacked inequality constrained objective function value is computed using eq.54. Finally, a gradient based sequential quadratic programming (SQP) solver is used to search iteratively the optimal continuous design parameters $\{T_k\}, \{\mathbf{d}_k\}, \{\boldsymbol{\mu}_{k-1}\}, \{\boldsymbol{\Sigma}_{k-1}\}$ and the slack variable $\{\kappa_k\}$. Algorithm I summarizes the searching procedure.

Algorithm 1 Optimization of Time-dependent TSP

```

1: procedure OPTIMIZE/TSP( $\mathbf{T}, \mathbf{I}$ )
2:   Input: Initial values of  $\{T_k\}, \{\mathbf{d}_k\}, \{\boldsymbol{\mu}_{k-1}\}, \{\boldsymbol{\Sigma}_{k-1}\}, \{\kappa_k\}$  and  $n_{iter}$ 
3:   Output: Optimal  $T_k^*, T_k^*$ , and  $\mathbf{d}_k^*$ 
4:    $iter = 0$ 
5:   while  $iter < n_{iter}$  or  $\nabla J > \epsilon$  do ▷ the optimal solution?
6:      $iter = iter + 1$ 
7:     for  $k$ th node do
8:        $\mathbf{x}_k \leftarrow \mathbf{f}(\mathbf{x}_{k-1})$ 
9:       propagate  $\boldsymbol{\mu}_{k|k-1}, \boldsymbol{\Sigma}_{k|k-1}$  of  $\bar{\mathcal{I}}_k$  ▷ eq.31- eq.32
10:      Propagate  $\boldsymbol{\mu}_{z,k}, \boldsymbol{\Sigma}_{z,k}$  of  $\bar{\mathcal{I}}_k$  ▷ eq.34 -eq.35
11:      Select an object  $\mathcal{I}_k$  from  $\mathbf{I}$  using priori with respect to  $\bar{\mathcal{I}}_k$  ▷ eq.24
12:      Characteristic parameters  $\mathbf{z}_k$  of  $\bar{\mathcal{I}}_k$ 
13:      Parameter of new cost function  $\boldsymbol{\mu}_{y,k}, \boldsymbol{\Sigma}_{y,k}$  of  $\bar{\mathcal{I}}_k$  ▷ eq.37-eq.38
14:       $y_k \leftarrow$  transfer cost of  $\mathcal{I}_k$ 
15:    end for
16:     $J \leftarrow$  objective function with the slack variable ▷ eq.54 - eq.55
17:    Update  $\{T_k\}, \{\mathbf{d}_k\}, \{\boldsymbol{\mu}_{k-1}\}, \{\boldsymbol{\Sigma}_{k-1}\}, \{\kappa_k\}$  using gradient based optimizer
18:  end while
19:  Return  $\{T_k\}, \{\mathcal{I}_k\}$  and  $\{\mathbf{d}_k\}$ 
20: end procedure

```

4 Test of Static TSP

Consider a test case of static TSP. The benchmark TSP consists of 14 points. Table 4 shows coordinates of the 14 points [23]. The objective of the problem is to find an optimal travel route such that each points is visited one and only once with the least possible distance traveled. Aravind Seshadri resolved this problem using a stochastic combinatorial optimization algorithm, Simulated Annealing (SA) algorithm [23].

Table 2 Coordinates of the points of TSP benchmark

ID	x	y
1	16.470	96.100
2	16.470	94.440
3	20.090	92.540
4	22.390	93.370
5	25.230	97.240
6	22.000	96.050
7	20.470	97.020
8	17.200	96.290
9	16.300	97.380
10	14.050	98.120
11	16.530	97.380
12	21.520	95.590
13	19.410	97.130
14	20.090	94.550

Different to the problem of optimizing tour of rendezvousing the debris, in test of benchmark, design variables are expected value and variance of x and y to be travelled to the next point. Candidate points are selected via analysing probabilities of possible candidates with the data set of parameter $\mu_x, \mu_y, \sigma_x, \sigma_y$. Table 4 shows the optimal solution of the benchmark using SA algorithm and corresponding design variables of μ_x, μ_y . Both starting point and final point are set to point 13. The minimum total cost of TSP is 30.8785.

Table 3 Optimal solutions of the benchmark

ID	μ_x	μ_y
13		
7	1.06	-0.11
12	1.05	-1.43
6	0.48	0.46
5	3.23	1.19
4	-2.84	-3.87
3	2.3	-0.83
14	0	2.01
2	-3.62	-0.11
1	0	1.66
10	-2.42	2.02
9	2.25	-0.74
11	0.23	0
8	0.67	-1.09
13		

Unlike the time-dependent TSP whose covariance of the node is predicted by numerical propagating differential equations, in the static TSP, variance of the position i , σ_i given prior variance of position i , σ_i^- (the variance parameter should be optimized) and variance at point $i - 1$, σ_{i-1} , variance at point i can

be computed as

$$\sigma_i^2 = (\sigma_i^-)^2 + \sigma_{i-1}^2 + 2\rho(\sigma_i^-)\sigma_{i-1} \quad (57)$$

where $\rho \in [0, 1]$ is the correlation factor. Candidate point i is selected using the distribution parameter $[\mu_{x,i}, \sigma_{x,i}]$ and $[\mu_{y,i}, \sigma_{y,i}]$.

Corresponding variance of distance $r_i = \sqrt{x_i^2 + y_i^2}$ of i th point can be computed as

$$\sigma_{r,i}^2 = \frac{(\sigma_{x,i}^2 \mu_{x,i}^2 + \sigma_{y,i}^2 \mu_{y,i}^2)}{(\mu_{x,i}^2 + \mu_{y,i}^2)}; \quad (58)$$

Therefore, the design variables for each point consists of the distribution parameters $\mu_x, \mu_y, \sigma_x, \sigma_y$, correlation factor ρ , and slack variable κ for the constraint to be met. Table 4 summarizes design variables of one point on the travel route. Total number of the design variables is therefore $7 \times 13 = 91$.

Table 4 Design variables of the static TSP

Parameters	Initial value	Lower bound	Upper bound
μ_x	-	-8.0	8.0
μ_y	-	8.0	6.5
σ_x	4.0	0.1	6.0
σ_y	4.0	0.1	6.0
ρ_x	0.2	0.0	1.0
ρ_y	0.2	0.0	1.0
κ	50	0.01	300

In this test, we provide two different constraints of the route. One is based on Chi-square threshold as the preceding section does. The objective function is set to minimize the total cost with chi-square constraints at each point

$$\min J = \sum_{i=1}^{14} r_i + \kappa_i \max(0, c_i) \quad (59)$$

where c_i is the inequality constraints at each point

$$c_i = (\mathbf{z}_i - \boldsymbol{\mu}_{z,i}) \boldsymbol{\Sigma}_{z,i}^{-1} (\mathbf{z}_i - \boldsymbol{\mu}_{z,i})^T + (r_i - \mu_{r,i}) \sigma_{r,i}^{-1} (r_i - \mu_{r,i})^T - \chi_n^2(\alpha) \quad (60)$$

and $\mathbf{z}_i = [x_i, y_i]$, $\boldsymbol{\mu}_{z,i} = [\mu_{x,i}, \mu_{y,i}]$, and $\boldsymbol{\Sigma}_{z,i} = \text{diag}([\sigma_{x,i}, \sigma_{y,i}])$ respectively.

Another one is based on Maximum A Posteriori (MAP) and can be written as

$$\min J = \sum_{i=1}^{14} r_i + \log(|\boldsymbol{\Sigma}_{z,i}|) + \log \sigma_{r,i} + (\mathbf{z}_i - \boldsymbol{\mu}_{z,i}) \boldsymbol{\Sigma}_{z,i}^{-1} (\mathbf{z}_i - \boldsymbol{\mu}_{z,i})^T + (r_i - \mu_{r,i}) \sigma_{r,i}^{-1} (r_i - \mu_{r,i})^T \quad (61)$$

In the equation of logarithm of posterior, items that have no influence to the optimal solution are removed.

Table 4 shows two groups of results obtained with different parameter settings. Initial values of $\mu_{x,i}$ and $\mu_{y,i}$ are given deterministically or randomly within a specific range near the optimal design variables, where $\mu_{x,i}^*$ and $\mu_{y,i}^*$ are the optimal design variables of $\mu_{x,i}$ and $\mu_{y,i}$, $\text{rnd} \in [0, 1]$ is a uniformly distributed random number in the interval $(0,1)$.¹

Table 5 Solutions with different initial parameter settings

Solution	Constraint	Initial value of $[\mu_{x,i}, \mu_{y,i}]$	Route	Cost
A	MAP	$[\mu_{x,i}^* + 1.0, \mu_{y,i}^* - 0.8]$	[13,7,12,6,5,4,3,14,2,1,10,9,11,8,13]	30.8785
B	Chi-square	$[-2 + 4\text{rnd}, -2 + 4\text{rnd}]$	[13,7,12,6,5,4,3,14,2,1,8,11,9,10,13]	31.567

It can be seen that if the initial values of design variables is within a certain neighbourhood of the optimal ones, one can obtain the global optimal solution directly using the single constraint of MAP. Regarding solution B, though the initial values are away from the optimal initial design parameters and randomly selected, the solutions obtained are still quite close to the global optimal solution.

With the numerical results, one can see that though the solution obtained is not necessarily global optimal for its gradient-based searching mechanism, however, because of the Chi-square inequality constraint at each point, convexity of the problem is improved (the inequality constraints can be written into equally into quadratic form equality constraints with Lagrange multiplier), and the more constraints the problem has, the more convex the problem can be, and the easier the optimizer could search the optimal route.

The proposed optimizer for the mixed integer TSP is designed assuming that the nodes are Gaussian correlated. The assumption looks reasonable in the test cases presented in the manuscript, but maybe too strict for some other TSP problems. We note that in the tests of TSP benchmark, within a specific range, given uniformly random distributed initial parameters, one can still find the near optimal solution. Therefore, if a more sophisticated distance measure other than Euclidean distance, and some more sophisticated correlation model can be given, generality of proposed approach could be improved. New sampling techniques and continuous stochastic constraints thresholds for the algorithm might help improve the algorithm's generality too. Such techniques for improving generality of proposed method in the future work are under considered.

5 Numerical simulation

Consider now a time-dependent multiple debris rendezvous problem. Ephemeris of the debris are from GTOC-9 website [14]. Table 6 summarizes distribution characteristics of the debris.

¹ Source code of the test of benchmark can be available at <https://github.com/Liqiang-Hou/Travelling-Salesman-Problem-of-Space-Trajectory-Design>

Table 6 Debris data set

	unit	mean value	standard deviation	maximum	minimum
semi-major axis, a	km	7131.6	58.503	7274.0	6996.1
eccentricity, e		0.0071438	0.004901	0.019318	0.00013122
inclination, inc	deg	98.415	0.84304	101.07	96.236
Ascending node Ω	deg	172.93	103.88	347.76	7.6191

5.1 Optimal solution of JPL

Table 7 shows the optimal solution of JPL using an improved genetic based evolutionary algorithm (GA). Initial branch and bound, beam search, and seeding combinatorial algorithms (Genetic Algorithm, GA) are used to search the optimal chain of rendezvous. A new structure genome, and heuristic adjustment are used to improve the GA. The optimal solution to remove the total 123 debris consist of 10 sequences. Table 7 shows one of the optimal sequences, its optimal transfer duration and costs of the sequence [20].

Table 7 Optimal solution of JPL

Parameter	Value
Start MJD2000	23557.18
End MJD2000	23821.03
Number of objectives	14
Debris ID	23,55,79,113,25,20,27,117,121,50,95,102,38,97
Transfer Duration, days	24.86,24.98,22.42,24.99,0.29,10.63,25.00, 2.70,1.51,1.41,24.67,24.31,5.86
Δv , m/s	161.8,139.2,65.8,208.2,115.2, 300.1,564.9,78.3,105.0,233.3, 453.5,340.4,300.8

5.2 Optimization of the sequence using continuous gradient optimizer

Consider the multiple debris rendezvous problem. Initial epoch and the first debris to remove of the mission is set to $MJD_0 = 23557$ and $\mathcal{I}_0 = 23$ as those of JPL.

Similar to JPL's solution, debris are selected and computed from the database of 123 debris, removal operation of the debris after each transfer is set to 5 days. As analyzed in preceding section, the expected value and covariance of expected debris \mathcal{I}_i^* , and ToF of each transfer are set to the parameters to be optimized. Table 8 shows the initial settings of the design parameters of each transfer. For each transfer, there are 10 design variables need to be optimized. The total number of the design parameters is therefore $14 \times 10 = 140$. The lower bound and upper bound of μ_Ω are set to -8^0 and 8^0 respectively as the maximum value of $\Delta\Omega$ obtained by varying Δa , Δi and

Δe of the debris is about 5^0 , corresponding upper bound of σ_Ω is set to 8^0 for the same reason.

Table 8 Parameter settings of the design parameters

Parameters	unit	lower bound	upper bound	initial value
T	days	0.5	25	20
μ_a	km	-150	150	0
μ_e		-1.0e-3	1.0e-3	0
μ_i	deg	-1.5	-1.5	0
μ_Ω	deg	-8.0	8.0	0
σ_a	km	5.0	50	30
σ_e		1.0e-4	1.0e-3	5.0e-4
σ_i	deg	0.1	1.0	0.5
σ_Ω	deg	0.1	8	5
κ		1.0e-3	300	50

The finite difference method is used to compute the Jacobian for covariance propagation. The Matlab[®] sequential quadratic programming (SQP) solver, fmincon is used to search the optimal sequence and ToF of the transfer. Table 9 shows parameter settings of the finite difference, fmincon optimizer and Chi-square threshold of the optimization.

Table 9 Parameter settings of the optimization

Parameter		unit	value
Finite difference for covariance propagation	δa	km	1.0e-2
	δe		1.0e-4
	δi	deg	1.0e-3
	$\delta \Omega$	deg	1.0e-3
Chi-square threshold			$\chi_2^2(0.98)$
Parameter settings of fmincon optimizer	TolX		1.0e-20
	TolFun		1.0e-20

5.3 Numerical results and analysis

First, a sequence of transfers with fixed ToF is optimized. The value of ToF is set to 20 days for each transfer between the debris. Figure 2 shows convergence history and three solutions of proposed algorithm. Table 10-Table 15 shows corresponding sequence, initial mean value and variance of the three solutions. Penalty of the cost function and velocity of each transfer are listed in the tables too. With the algorithm, it takes couples of iterations to reduce the penalties of transfer cost sufficiently close to zero. Variance and mean value of the sequence orbital elements converge also to a sufficient low level.

The gradient based optimizer, fmincon of Matlab[®] is again used to refine the ToF of each transfer of the sequence. Table 16 summarizes the optimal

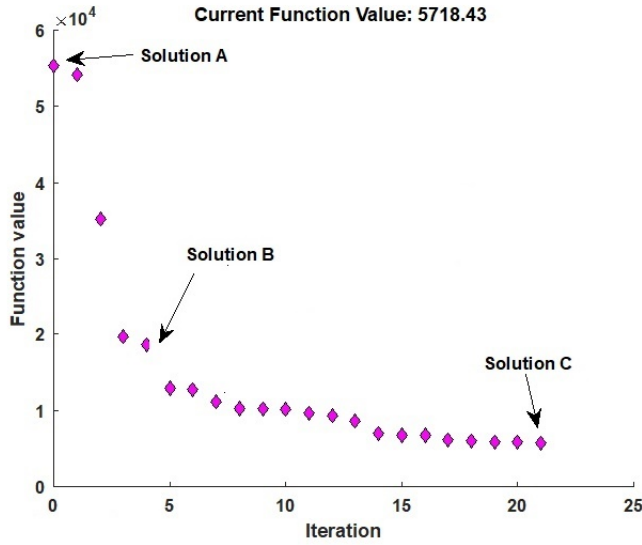


Fig. 2 Convergence history

solution of the sequence. A sequence of total $\Delta V = 3337.0\text{m/s}$ is obtained, while the total cost of JPL is 2966.5m/s . In this test, analytical approximation formulas are used to compute the transfer cost, while in JPL's results, a global multiple shooting based local optimization with numerical orbital propagator is used. Considering accuracy level of the two models used, the costs of two test sequences can be seen at similar level.

From the tables, it can be seen that with proposed algorithm, both the mean value and variances of the orbital parameters converge gradually to appropriate values that associate to the IDs of targets. However, the variance of semi-major axis, σ_a remains almost unvaried. This is due to the impact of the semi-major axis to the ΔV . Given a variation of semi-major axis $\Delta a = 30\text{km}$, the ΔV varied due to Δa is about 15m/s , while for the ascending node and inclination, this value could be up to more than 100m/s if $\Delta\Omega$ and Δi are set to 1° respectively (eq.14-eq.17). Therefore, the value of σ_a varies significantly less than other design parameters during the optimization.

One can also see that, though the design parameter of ToF and sequence can be optimized directly following the algorithm, in this test, a two-step strategy is used to search the optimal solution of the sequence. First, an optimal sequence with fixed-ToF is determined, a local optimizer is then used to search optimal ToF and ΔV for each transfer. Since the ToFs are not considered in the first step, some actual optimal solutions may be missed during the optimization. The reason that the two-step strategy is used is related to the covariance and cost function propagation strategy in the optimization. In this test, the first-order approximation for the covariance propagation is used. The state equation of orbital elements are highly nonlinear. Transition matrix of

the states of orbital elements can not be given explicitly, the finite difference is therefore used to compute indirectly the covariance due to varied states. For the similar reason, it is hard to propagate the covariance by integrating the Ricatti equation in which an explicit state transition matrix is required. Therefore, the fixed ToF optimization is used to avoid the complex varied time-step covariance propagation. With the approximation, one needs to tune carefully the finite difference of the covariance propagation, and optimality of the solutions is dependent on the finite difference used.

We note the recent sigma-point technique for covariance propagation. With sigma-point technique, covariance of the state and observation can be propagated directly using the nonlinear state and observation equations. Such a work that directly optimizes the sequence using derivative-free covariance propagation will be included in future work. A state equation with position and velocity will also be considered, in which the state transition matrix can be explicitly listed. In this test, part of the orbital elements related design variables, e.g. σ_Ω is quite insensitive to the varied cost function values. If design variables of position vectors are introduced, sensitivity of the design variables to the varied cost function will be improved.

Table 10 Solution A: the sequence

Penalty	Tof(days)	Delta V(km/s)	\mathcal{I}_{k-1}	\mathcal{I}_k
3833.6	20	0.33356	23	55
3630.9	20	0.33285	55	113
4109	20	0.19693	113	121
2515.4	20	0.59675	121	117
3921	20	0.30597	117	79
3694	20	0.34758	79	20
3720.5	20	0.3394	20	25
4107.9	20	0.18808	25	27
3848.2	20	0.26756	27	84
4202.1	20	0.71163	84	83
4038.2	20	0.96796	83	50
3948.4	20	0.6506	50	118
3282.8	20	0.41598	118	95
2364.2	20	0.63115	95	87

6 Conclusions

The time-dependent TSP problem is hard to resolve due to its complicated design space structure. Conventional combinatorial algorithms such as search tree and seeding combinatorial algorithms use selection and regenerating operators based on the integer type variables. Efficiency of the searching procedure is highly dependent on the policy used for the integer based operation.

Different to the conventional TSP methods, the new algorithm resolves the problem using a gradient based search. A probabilistic mapping is intro-

Table 11 Solution A: mean value and variance

μ_a (km)	μ_i (deg)	μ_o (deg)	σ_a (km)	σ_i (deg)	σ_o (deg)	μ_v (km/s)	σ_v (km/s)
0	0	0	30	1	3	0	0.33976
0	0	0	30	1	3	0	0.34934
0	0	0	30	1	3	0	0.34984
0	0	0	30	1	3	0	0.35219
0	0	0	30	1	3	0	0.3603
0	0	0	30	1	3	0	0.35758
0	0	0	30	1	3	0	0.34931
0	0	0	30	1	3	0	0.36707
0	0	0	30	1	3	0	0.33538
0	0	0	30	1	3	0	0.3365
0	0	0	30	1	3	0	0.35832
0	0	0	30	1	3	0	0.32785
0	0	0	30	1	3	0	0.34322
0	0	0	30	1	3	0	0.34184

Table 12 Solution B: the sequence

Penalty	Tof(days)	Delta V(km/s)	\mathcal{I}_{k-1}	\mathcal{I}_k
193.76	19.984	0.33333	23	55
526.91	19.984	0.33294	55	113
1.9254	19.984	0.096311	113	79
193.8	19.984	0.29176	79	121
741.25	19.983	0.42998	121	117
632.04	19.984	0.49426	117	57
611.02	19.99	0.69273	57	20
737.28	20.003	0.47951	20	27
217.48	20.003	0.26803	27	84
0.96473	20.002	0.11276	84	83
30.334	20.002	0.265	83	50
94.584	20.003	0.25041	50	118
412.72	20.005	0.34214	118	25
910.09	20.006	0.54754	25	95

duced to associated the integer ID to continuous characteristic parameters. Parameter estimation techniques such as covariance propagation are used to determine the optimal characteristic parameters. No tree or graph based operation is involved. Though the optimizer is designed using stochastic techniques, the searching procedure is implemented deterministically. **Chi-square threshold checking operation is introduced into the optimization, and used to improve convexity of the problem.**

Another contribution of the strategy is from the Baseysin based heuristics. Stochastic meta heuristics are commonly used in prevalent TSP algorithms. In these algorithms, individuals and branches are generated and sampled using probabilistic heuristic, but few of them uses Bayesian based response analysis directly in the operations due to the discrete and mixed integer nature. With the continuous mapping and Bayesian analysis, objective function of the sequence is reformulated into a continuous quadratic-like search problem. As

Table 13 Solution C: mean value and variance

μ_a (km)	μ_i (deg)	μ_o (deg)	σ_a (km)	σ_i (deg)	σ_o (deg)	μ_v (km/s)	σ_v (km/s)
80.241	0.20271	0.25162	29.691	0.59927	2.5142	0.057949	0.1238
68.961	0.14367	0.1659	29.777	0.33223	2.4502	0.052913	0.10902
6.9494	0.019553	0.071687	29.997	0.4815	2.6018	0.011746	0.14774
56.518	0.13509	0.16085	29.701	0.65134	2.4081	0.03901	0.12259
117.79	0.30928	0.37205	29.353	0.45844	2.4847	0.084661	0.11743
171.14	0.39852	0.45827	29.379	0.52076	2.4762	0.15569	0.11906
219.99	0.54225	0.63295	29.624	0.30007	2.46	0.1493	0.11256
143.58	0.37154	0.43753	29.338	0.49681	2.4938	0.10586	0.12098
52.673	0.13962	0.17868	29.706	1.2963	2.5114	0.036761	0.18234
10.65	0.029357	0.09848	29.985	0.48589	2.3233	0.013828	0.12152
56.707	0.14237	0.16824	29.805	0.67806	2.5316	0.052932	0.13629
46.089	0.07849	0.0956	29.919	0.37909	2.5339	0.043194	0.11532
76.403	0.15493	0.17917	29.827	0.36931	2.4881	0.061738	0.11272
179.85	0.44911	0.55832	29.189	0.49114	2.518	0.12415	0.11769

Table 14 Solution C: sequence

Penalty	Tof(days)	Delta V(km/s)	\mathcal{I}_{k-1}	\mathcal{I}_k
0	20	0.33365	23	55
0.43601	20	0.33282	55	113
0	20	0.096486	113	79
0.76409	20	0.29294	79	121
0.33184	20	0.42921	121	117
0	20	0.4898	117	57
0	20	0.68889	57	20
0.59349	20	0.47947	20	27
0.85352	20	0.26742	27	84
0	20	0.11133	84	83
0.94618	20	0.2685	83	50
0.90029	20	0.25063	50	118
0.64101	20	0.34123	118	25
0	20	0.54873	25	95

far as the authors know, the research study is the first trial in space mission design to employ a continuous gradient optimizer to resolve mixed integer time-dependent space TSP.

The method is designed stochastically in essence, a robust design of TSP considering uncertainty impact using the proposed method can be considered in future work. Extensions and application of the proposed algorithm to the TSP with multiple objectives are well worth trying too. Applications of the continuous mapping and Bayesian mechanism to the multi-target flybys and multi-gravitational assist are also considered.

Acknowledgements This work is supported by National Natural Science Foundation of China, No.U20B2056,U20B2054.

Table 15 Solution C: mean value and variance

μ_a (km)	μ_i (deg)	μ_o (deg)	σ_a (km)	σ_i (deg)	σ_o (deg)	μ_v (km/s)	σ_v (km/s)
53.706	0.16283	1.656	19.688	0.31928	0.36124	0.22875	0.016381
41.364	0.19485	1.4922	19.268	0.56979	1.8124	0.23917	0.10725
-12.849	0.28146	2.4948	18.348	0.36068	0.83147	0.46402	0.039063
40.8	-0.068711	-0.52225	20.063	0.68693	2.1619	0.15941	0.13708
77.781	0.16261	1.2189	18.847	0.56092	1.5637	0.15396	0.083502
138.13	0.031337	1.3298	18.45	0.35088	0.92499	0.075472	0.015769
146.61	0.17877	1.1054	19.041	0.47357	1.6726	0.12666	0.070588
96.794	0.15679	1.0286	18.981	0.6832	2.1857	0.11309	0.14058
32.133	0.041496	0.3307	19.331	0.75819	3.4516	0.031035	0.26005
-30.017	0.4219	2.8362	13.339	0.51202	0.79282	0.5873	0.057609
37.748	0.15001	0.88379	19.886	0.78621	7.9787	0.13354	1.1676
25.887	0.10616	0.77631	19.589	0.82071	4.1815	0.11944	0.38334
47.493	0.14112	1.0868	19.514	0.60612	2.1292	0.15945	0.12676
120.86	0.11869	0.84214	18.596	0.5103	1.7112	0.065413	0.028208

Table 16 Optimal sequence

Parameter	unit	Value
ID		23, 55, 113, 79, 121, 117, 57, 20, 27, 84, 83, 50, 118, 25,95
Tof	days	8.5433, 24.966, 19.166, 24.964, 24.994, 24.989, 24.996, 23.834, 21.521, 5.0216, 14.567, 24.986, 24.989
ΔV	m/s	160.38, 351.14, 77.365, 261.65, 411.83, 245.97, 370.18, 475.27, 184.97, 77.182, 192.64, 255.65, 272.76
Total ΔV	m/s	3337.0

References

1. Abdelkhalik, O., Gad, A.: Dynamic-size multiple populations genetic algorithm for multigravity-assist trajectory optimization. *Journal of Guidance, Control, and Dynamics* **35**(2), 520–529 (2012). DOI 10.2514/1.54330. URL <https://doi.org/10.2514/1.54330>
2. Browne, C., Powley, E.J., Whitehouse, D., Lucas, S.M., Cowling, P.I., Rohlfshagen, P., Tavener, S., Perez, D., Samothrakis, S., Colton, S.: A survey of monte carlo tree search methods. *IEEE Transactions on Computational Intelligence and AI in Games* **4**(1), 1–43 (2012)
3. Cerf, M.: Multiple space debris collecting mission: optimal mission planning. *Journal of Optimization Theory and Applications* **167**(1), 195–218 (2015)
4. Ceriotti, M., Vasile, M.: Mga trajectory planning with an aco-inspired algorithm. *Acta Astronautica* **67**(9), 1202–1217 (2010)
5. Daneshjou, K., Mohammadi-Dehabadi, A., Bakhtiari, M.: Mission planning for on-orbit servicing through multiple servicing satellites: A new approach. *Advances in Space Research* **60**(6), 1148–1162 (2017)
6. Deb, K., Padhye, N., Neema, G.: Interplanetary trajectory optimization with swing-bys using evolutionary multi-objective optimization. In: L. Kang, Y. Liu, S. Zeng (eds.) *Advances in Computation and Intelligence*, pp. 26–35. Springer Berlin Heidelberg, Berlin, Heidelberg (2007)
7. Deb, K., Padhye, N., Neema, G.: Interplanetary trajectory optimization with swing-bys using evolutionary multi-objective optimization. In: L. Kang, Y. Liu, S. Zeng (eds.) *Advances in Computation and Intelligence*, pp. 26–35. Springer Berlin Heidelberg, Berlin, Heidelberg (2007)

8. Di Carlo, M., Martin, J.M.R., Vasile, M.: Automatic trajectory planning for low-thrust active removal mission in low-earth orbit. *Advances in Space Research* **59**(5), 1234–1258 (2017)
9. Federici, L., Zavoli, A., Colasurdo, G.: Impulsive multi-rendezvous trajectory design and optimization. In: 8th European Conference for Aeronautics and Space Sciences (2019)
10. Gad, A., Abdelkhalik, O.: Hidden genes genetic algorithm for multi-gravity-assist trajectories optimization. *Journal of Spacecraft and Rockets* **48**(4), 629–641 (2011). DOI 10.2514/1.52642. URL <https://doi.org/10.2514/1.52642>
11. Heaton, A., Strange, N.J., Longuski, J.M., Bonfiglio, E.: Automated design of the europa orbiter tour. *Journal of Spacecraft and Rockets* **39**(1), 17–22 (2002)
12. Hennes, D., Izzo, D.: Interplanetary trajectory planning with monte carlo tree search. In: Twenty-Fourth International Joint Conference on Artificial Intelligence (2015)
13. Izzo, D., Maertens, M.: The kessler run: On the design of the gtoc9 challenge. *Acta Futura* **11**, 11–24 (2018). DOI 10.5281/zenodo.1139022. URL <https://doi.org/10.5281/zenodo.1139022>
14. Izzo, D., Simoes, L.F., Yam, C.H., Biscani, F., Di Lorenzo, D., Addis, B., Cassioli, A.: Gtoc5: Results from the european space agency and university of florence. *Acta Futura* **8**, 45–55 (2014). URL <http://dx.doi.org/10.2420/AF08.2014.45>
15. Julier, S.J.: The scaled unscented transformation. In: Proceedings of the 2002 American Control Conference (IEEE Cat. No. CH37301), vol. 6, pp. 4555–4559. IEEE (2002)
16. Longuski, J.M., Williams, S.N.: Automated design of gravity-assist trajectories to mars and the outer planets. *Celestial Mechanics and Dynamical Astronomy* **52**(3), 207–220 (1991)
17. Murakami, J., Hokamoto, S.: Approach for optimal multi-rendezvous trajectory design for active debris removal. In: 61th International Astronautical Congress,(pp. IAC-10. C1. 5.8). Prague, CZ (2010)
18. Nyew, H.M., Abdelkhalik, O., Onder, N.: Structured-chromosome evolutionary algorithms for variable-size autonomous interplanetary trajectory planning optimization. *Journal of Aerospace Information Systems* **12**(3), 314–328 (2015). DOI 10.2514/1.I010272. URL <https://doi.org/10.2514/1.I010272>
19. Petropoulos, A., Longuski, J.M., Bonfiglio, E.: Trajectories to jupiter via gravity assists from venus, earth, and mars. *Journal of Spacecraft and Rockets* **37**(6), 776–783 (2000)
20. Petropoulos, A.E., Bonfiglio, E.P., Grebow, D.J., Lam, T., Parker, J.S., Arrieta, J., Landau, D.F., Anderson, R.L., Gustafson, E.D., Whiffen, G.J., Finlayson, P.A., Sims, J.A.: Gtoc5: Results from the jet propulsion laboratory. *Acta Futura* **8**, 21–27 (2014). URL <http://dx.doi.org/10.2420/AF08.2014.21>
21. Pichugina, O., Yakovlev, S.: Continuous representation techniques in combinatorial optimization. *IOSR Journal of Mathematics* **13**(2), 12–25 (2017)
22. Pichugina, O.S., Yakovlev, S.V.: Continuous representations and functional extensions in combinatorial optimization. *Cybernetics and Systems Analysis* **52**(6), 921–930 (2016). DOI 10.1007/s10559-016-9894-2. URL <https://doi.org/10.1007/s10559-016-9894-2>
23. Seshadri, A.: Aravind seshadri (2021). traveling salesman problem (tsp) using simulated annealing, matlab central file exchange. retrieved jan 21, 2021. (2021). URL <https://www.mathworks.com/matlabcentral/fileexchange/9612-traveling-salesman-problem-tsp-using-simulated-annealing>
24. Simões, L.F., Izzo, D., Haasdijk, E., Eiben, A.: Multi-rendezvous spacecraft trajectory optimization with beam p-aco. In: European Conference on Evolutionary Computation in Combinatorial Optimization, pp. 141–156. Springer (2017)
25. Stuart, J., Howell, K., Wilson, R.: Application of multi-agent coordination methods to the design of space debris mitigation tours. *Advances in Space Research* **57**(8), 1680–1697 (2016)
26. Stuart, J.R., Howell, K.C., Wilson, R.S.: Design of end-to-end trojan asteroid rendezvous tours incorporating scientific value. *Journal of Spacecraft and Rockets* **53**(2), 278–288 (2016)
27. Tsirogiannis, G.A.: A graph based methodology for mission design. *Celestial Mechanics and Dynamical Astronomy* **114**(4), 353–363 (2012)
28. Vasile, M., Martin, J.M.R., Masi, L., Minisci, E., Epenoy, R., Martinot, V., Baig, J.F.: Incremental planning of multi-gravity assist trajectories. *Acta Astronautica* **115**, 407–421 (2015)

-
29. Yu, J., Chen, X.q., Chen, L.h.: Optimal planning of leo active debris removal based on hybrid optimal control theory. *Advances in Space Research* **55**(11), 2628–2640 (2015)